

Orbital Motion in Pre-Main Sequence Binaries

Gail H. Schaefer¹, Lisa Prato², Michal Simon³, and Jenny Patience^{4,5}

¹The CHARA Array of Georgia State University, ²Lowell Observatory, ³Stony Brook University, ⁴Arizona State University, ⁵University of Exeter

Abstract

We present results from our ongoing program to map the orbits of pre-main sequence binaries in the Taurus star forming region using adaptive optics imaging at the Keck Observatory. Our goal is to measure precise masses of young, low-mass stars to compare with models of stellar evolution. Our current findings are summarized below:

(i) Definitive orbits computed for V807 Tau Ba-Bb (Schaefer et al. 2012) and NTTs 045251+3016 (Simon et al. 2013).

(ii) Preliminary orbit solutions for DF Tau, T Tau Sa-Sb, and ZZ Tau. The parameters presented for these orbits are likely to be revised with additional measurements in the future.

(iii) Seven systems show curvature or acceleration in their relative motion. We can place lower limits on their orbital periods. Full solutions will be possible as we obtain more coverage of their orbits.

(iv) Five systems show motion that is indistinguishable from linear motion. The small relative motion between the components (< 6 mas/yr) suggests that these systems are bound. Simulations suggest that $\sim 20\%$ of orbits drawn randomly from a sample ($P=5-500$ yr, $a=30-1000$ mas) will have separations between 30-350 mas and show linear motion over a time-frame of 20 yr. Additional observations will confirm whether these systems are bound.

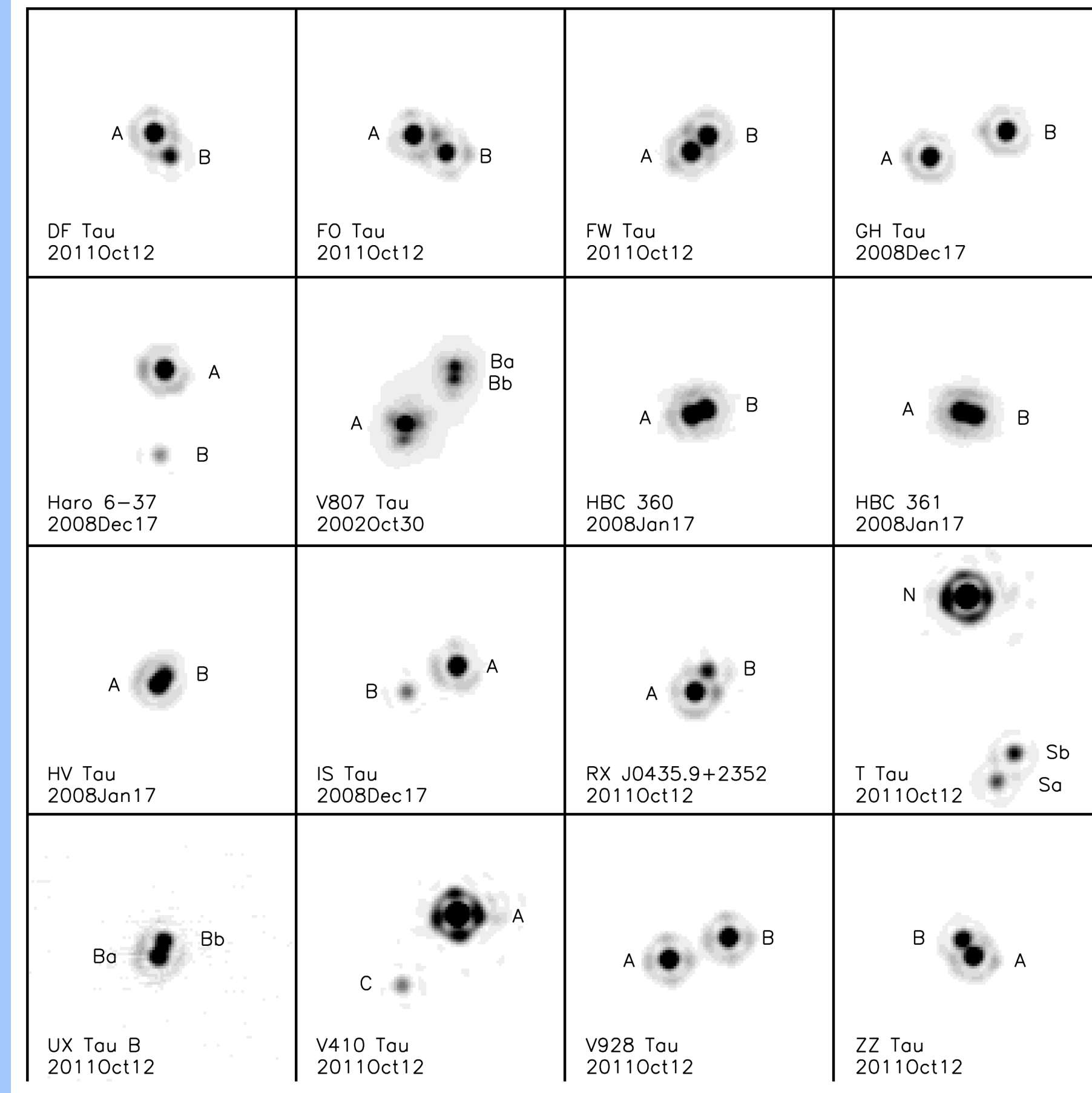
Adaptive Optics Imaging

Figure 1: Keck NIRC2 adaptive optics (AO) images of binaries in the Taurus star forming region. Each panel is 1" wide. Wide companions with separations larger than 1" are not shown.

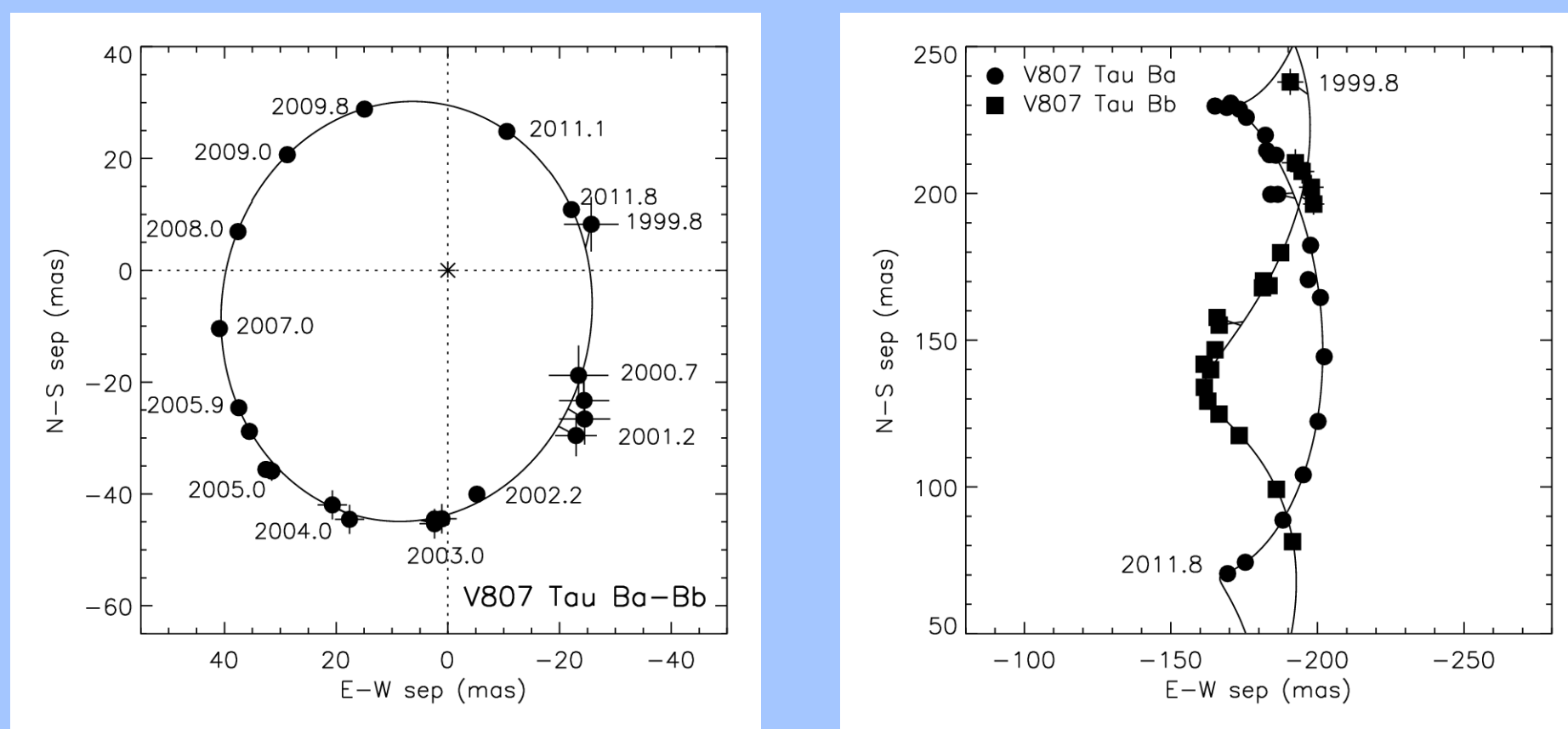
Our sample consists of known binaries with separations between 30-350 mas. We have been monitoring their orbital motion over the past decade using adaptive optics imaging. We combined our measurements with previous positions published in the literature and show the current status of orbital motion observed for each binary.

Reference Codes for Previously Published Measurements

Ba02 Balega et al. 2002, A&A, 385, 87
Ba04 Balega et al. 2004, A&A, 422, 627
Ba07 Balega et al. 2007, Ast Bull, 62, 339
Be04 Beck et al. 2004, ApJ, 614, 225
Ch90 Chen et al. 1990, ApJ, 357, 224
Co06 Correia et al. 2006, A&A, 459, 909
Du99 Duchene 1999, A&A, 341, 547
Du02 Duchene et al. 2002, ApJ, 568, 771
Du05 Duchene et al. 2005, A&A, 438, 769
Du06 Duchene et al. 2006, A&A, 457, L9
Du10 Duchene et al. 2010, ApJ, 712, 112
Fu03 Furlan et al. 2003, ApJ, 596, L87
Gh93 Ghez et al. 1993, AJ, 106, 2005
Gh95 Ghez et al. 1995, AJ, 110, 753
HK03 Hartigan & Kenyon 2003, ApJ, 583, 334
K94 Kenyon et al. 1994, AJ, 108, 1872
KL98 Kohler & Leiner 1998, A&A, 331, 977
Kl00 Kohler et al. 2000, IAU Symp, 200, 63
Kl08 Kohler et al. 2008, A&A, 482, 929
K000 Koresko 2000, ApJ, 531, L147
KH12 Kraus & Hillenbrand 2012, AJ, 134, 2340
Kr11 Kraus et al. 2011, ApJ, 731, 8
Lei91 Leiner et al. 1991, A&A, 250, 407
Lei93 Leiner et al. 1993, A&A, 278, 129
Ma06 Mayama et al. 2006, PASJ, 58, 375
MB00 Morin & Bouvier 2000, A&A, 356, L75
Ra09 Ratzka et al. 2009, A&A, 502, 623
Ri99 Richichi et al. 1999, A&A, 346, 501
Sc03 Schaefer et al. 2003, AJ, 126, 1971
Sc06 Schaefer et al. 2006, AJ, 132, 2618
Sc12 Schaefer et al. 2012, ApJ, 756, 120
Sh06 Shakovskij et al. 2006, A&A, 448, 1075
S92 Simon et al. 1992, ApJ, 384, 212
S96 Simon et al. 1996, ApJ, 469, 890
S95 Simon et al. 1995, ApJ, 443, 625
S13 Simon et al. 2013, ApJ, in press
Sk08 Skemer et al. 2008, ApJ, 676, L082
St01 Steffen et al. 2001, AJ, 122, 997
Ta02 Tamazian et al. 2002, ApJ, 578, 925
Th95 Thiebaud et al. 1995, A&A, 304, L17
W0101 White & Ghez 2001, A&A, 556, 265
W0102 White & Ghez 2001, A&A, 369, 249

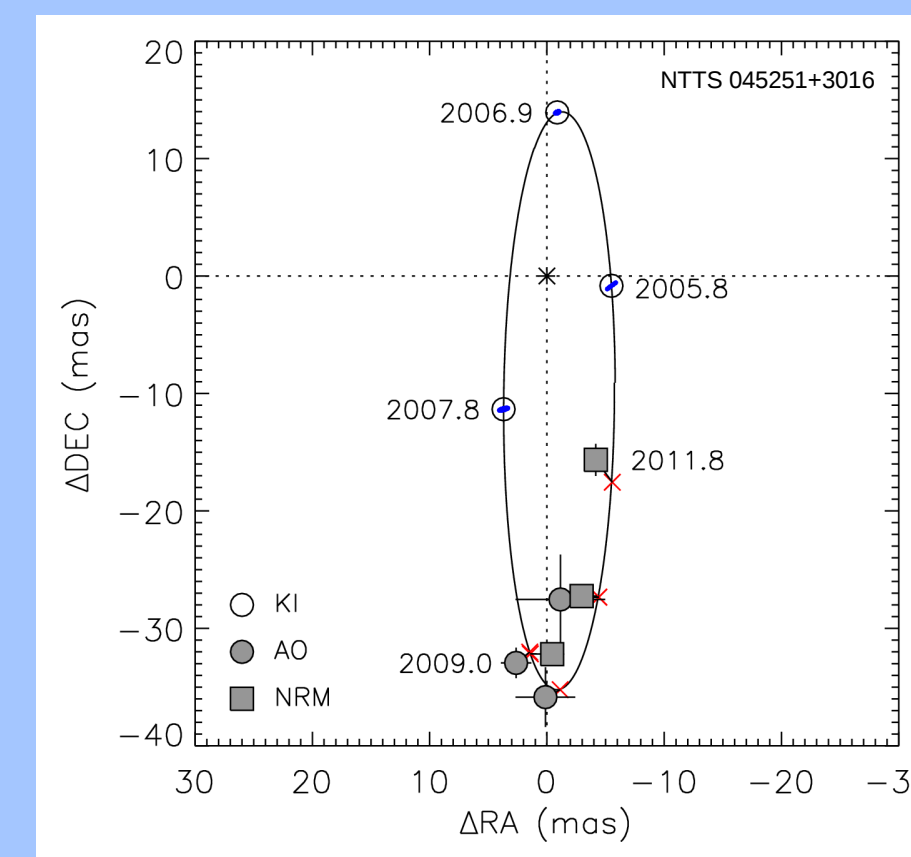


V807 Tau (Elias 12)



Completed Orbits

Parameter	V807 Tau Ba-Bb	NTTs 045251+3016
P (yr)	12.31 ± 0.06	6.882 ± 0.008
T	1991.15 ± 0.07	2000.23 ± 0.03
e	0.292 ± 0.003	0.494 ± 0.007
a (mas)	38.59 ± 0.16	25.57 ± 0.12
i ($^\circ$)	151.6 ± 0.9	78.1 ± 1.0
Ω ($^\circ$)	1.8 ± 1.6	178.1 ± 0.8
ω ($^\circ$)	50.6 ± 1.3	213.0 ± 1.7
M_1 (M_\odot)	0.56 ± 0.02 ($d/140\text{pc}$) ³	0.86 ± 0.11
M_2 (M_\odot)	0.48 ± 0.02 ($d/140\text{pc}$) ³	0.55 ± 0.05
d (pc)	140 (fixed)	158.7 ± 3.9



NTTs 045251 +3016

Figure 3 - Left: Orbital motion of V807 Tau Bb relative to Ba based on our NIRC2 AO images and data from the FGS on HST (Sc03, Sc06, Sc12). The visual orbit gives a total mass $1.04 M_\odot$ at the average distance to the Taurus star forming region of 140 pc (K94). Right: By modeling the astrometric center of mass motion of the components in the close pair relative to the wide component, V807 Tau A, we measured a mass ratio of 0.843 for Ba/Bb. Combining the results we derive the individual masses listed in the table on the right. We are working on measuring a precise parallax to the system using the VLBA (Schaefer et al. 2012).

Figure 4 - Left: Orbital motion for NTTs 045251+3016 based on NIRC2 AO (grey circles) and aperture masking (squares). The computed positions during the epochs of archived Keck Interferometer observations are marked by open circles. Right: Radial velocities from Steffen et al. (2001) and Simon (2013). Visible observations are shown in black and IR in red. We computed a simultaneous orbit to the AO, aperture masking, interferometric visibilities, and spectroscopic radial velocities. Combining the radial velocity amplitudes with the orbital parameters in the table on the left, we derived individual masses and an independent distance to the system (Simon et al. 2013).

Preliminary Orbit Solutions

Binary	P (yr)	T	e	a (mas)	i ($^\circ$)	Ω ($^\circ$)	ω ($^\circ$)	M_{tot} (M_\odot)
DF Tau A-B	41.3 ± 3.7	1981.4 ± 1.9	0.340 ± 0.091	93.3 ± 1.2	141.9 ± 4.1	22.7 ± 8.3	296.7 ± 8.8	1.30 ± 0.22
T Tau Sa-Sb	28.0 ± 4.2	1995.6 ± 1.0	0.52 ± 0.14	86.8 ± 8.7	25.4 ± 18.0	104.3 ± 30.2	38.0 ± 23.9	2.67 ± 0.29
ZZ Tau A-B	46.4 ± 3.4	1995.04 ± 0.30	0.569 ± 0.032	87.0 ± 5.8	124.4 ± 2.4	136.9 ± 2.3	295.1 ± 2.6	0.84 ± 0.21

Orbits Showing Curvature and Linear Motion

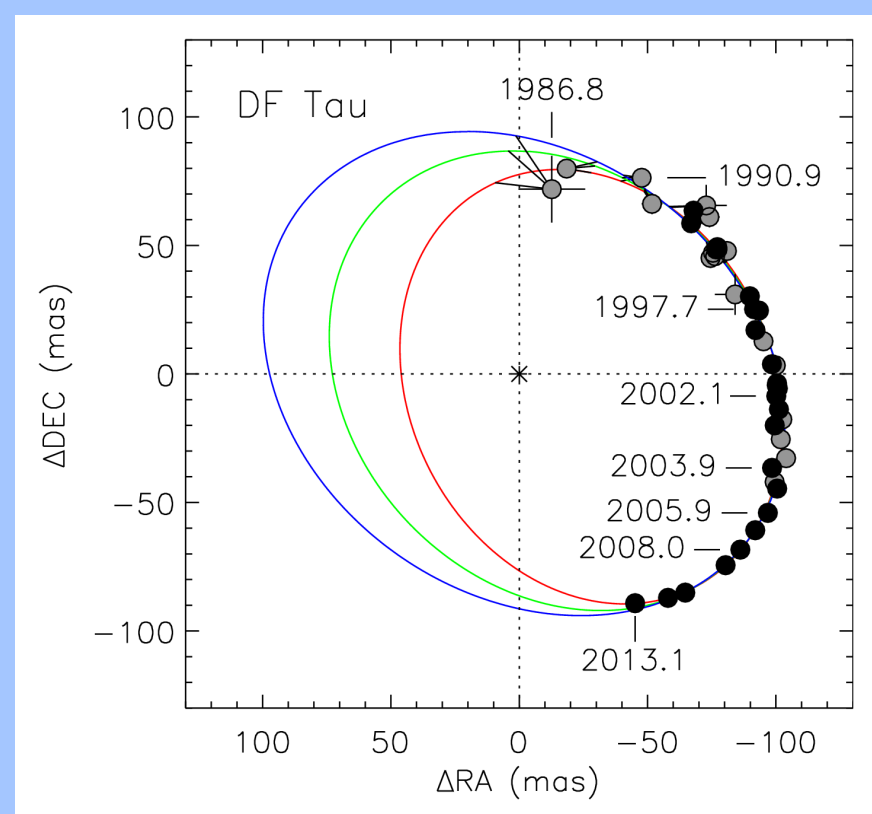


Figure 5 - Orbital motion for DF Tau. Black circles are our NIRC2 measurements. Grey circles are from the literature (Ch90, Gh95, Th95, WG01, Ba02, Ba04, Ba07, Sh06). A formal fit yields an orbital period of 41 yr. Overplotted are orbits at periods of 40 (red), 50 (green), and 60 yr (blue) to demonstrate that longer orbital periods could be possible.

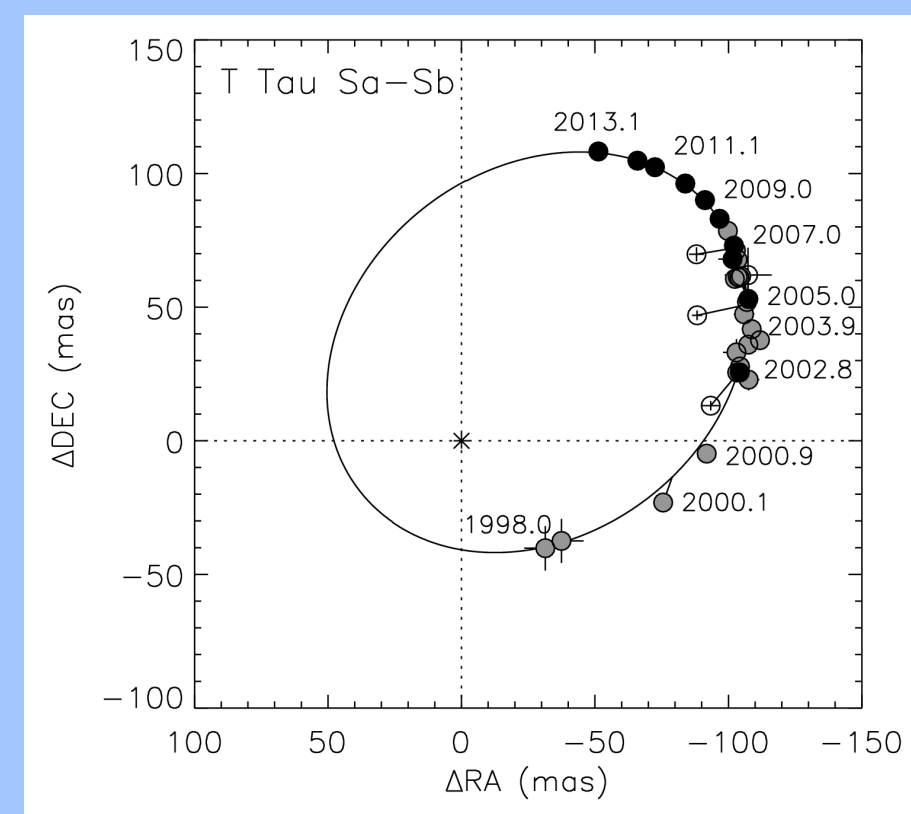


Figure 6 - Orbital motion for T Tau Sa-Sb. Black circles are our NIRC2 measurements. Grey circles are from the literature (Kh00, K000, Du02, Fu03, Be04, Du05, Du06, Ma06, Sc06, Kh08, Sk08, Ra09). Overplotted is the best fit orbit with a period of 28 yr. T Tau N is located 7" to the north. Duchene et al. (2006) and Kohler et al. (2008) present preliminary orbits that include the relative motion of all three components.

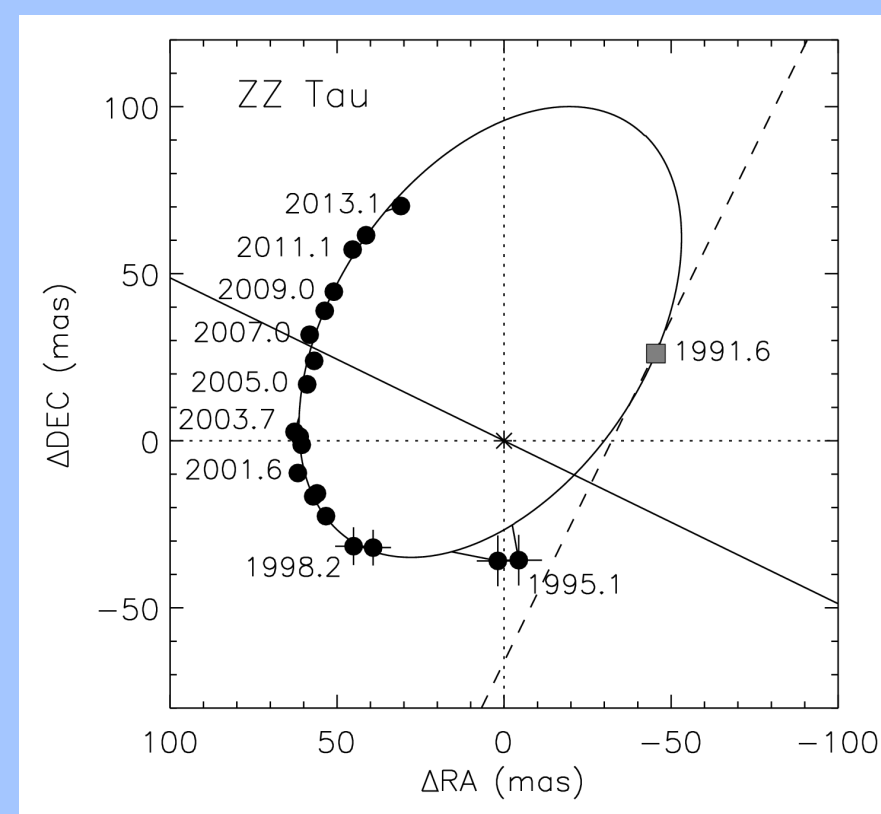


Figure 7 - Orbital motion for ZZ Tau. Black circles are our NIRC2 measurements and FGS observations (Sc03, Sc06). The solid line shows the direction of the lunar occultation in S95 and the dashed line shows the measured projected separation of 29 mas. The orbit must intersect this line. Overplotted is the best-fit orbit with a period of 46 yr. The position in the orbit at the time of the lunar occultation is marked by the shaded square.

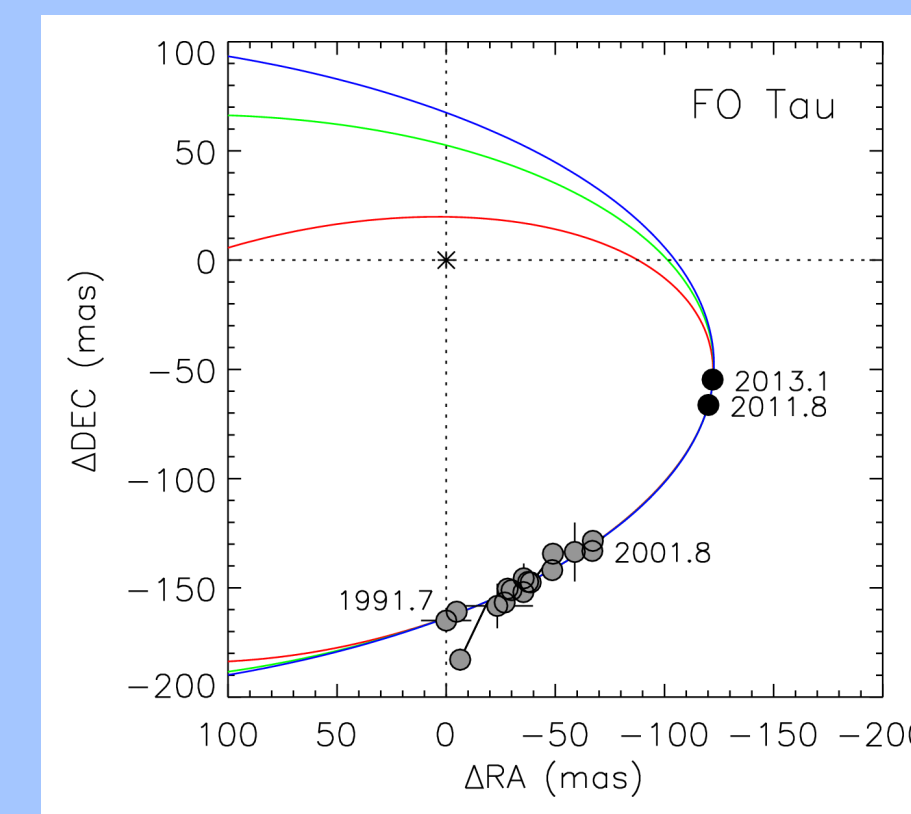


Figure 8 - Orbital motion for FO Tau. Black circles are our NIRC2 measurements. Grey circles are published values from the literature (Lei93, Gh95, WG01, HK03, Ta02). Overplotted are three example orbits at periods of 100 (red), 200 (green), and 300 yr (blue) that are consistent with the observed motion. A statistical analysis of orbital solutions that fit the data indicates that $P > 44$ yr.

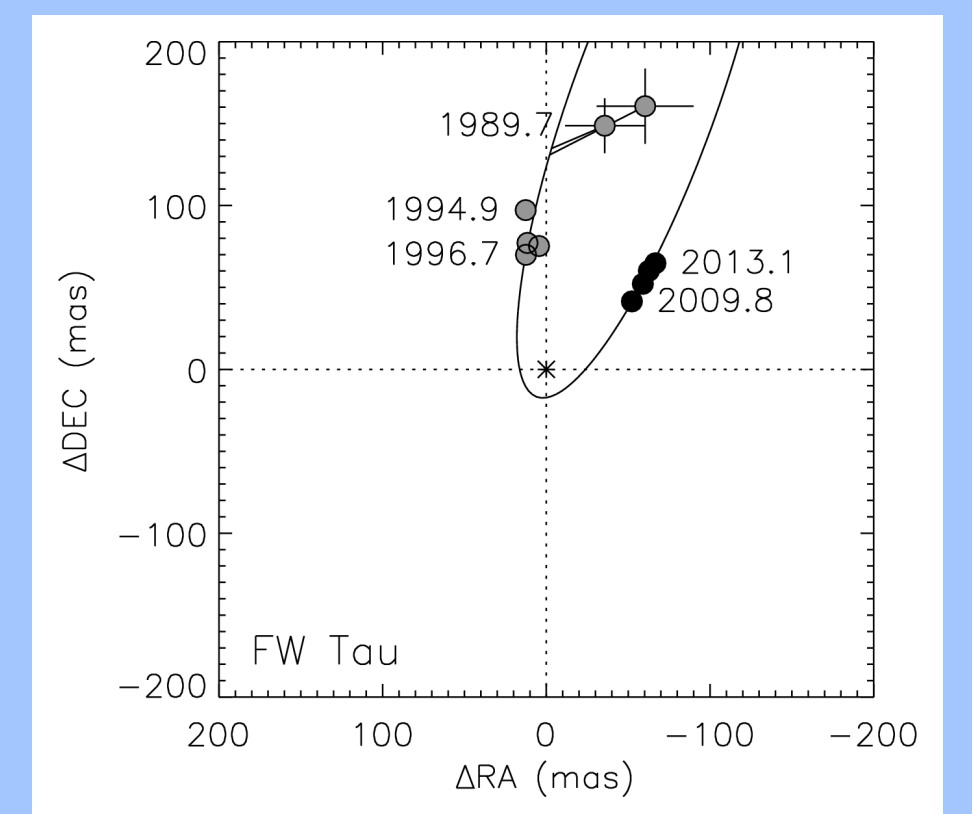


Figure 9 - Orbital motion for FW Tau. Black circles are our NIRC2 measurements. Grey circles are from the literature (Ch90, Lei91, S92, W0101, WG01). The example orbit has a period of 200 yr. The components are nearly equal brightness, so if we flip the position angle of the early measurements by 180° , then we get a solution showing linear motion, but the quality of the fit isn't as good. In either scenario, a statistical analysis of orbital solutions that fit the data indicates that $P > 40$ yr.

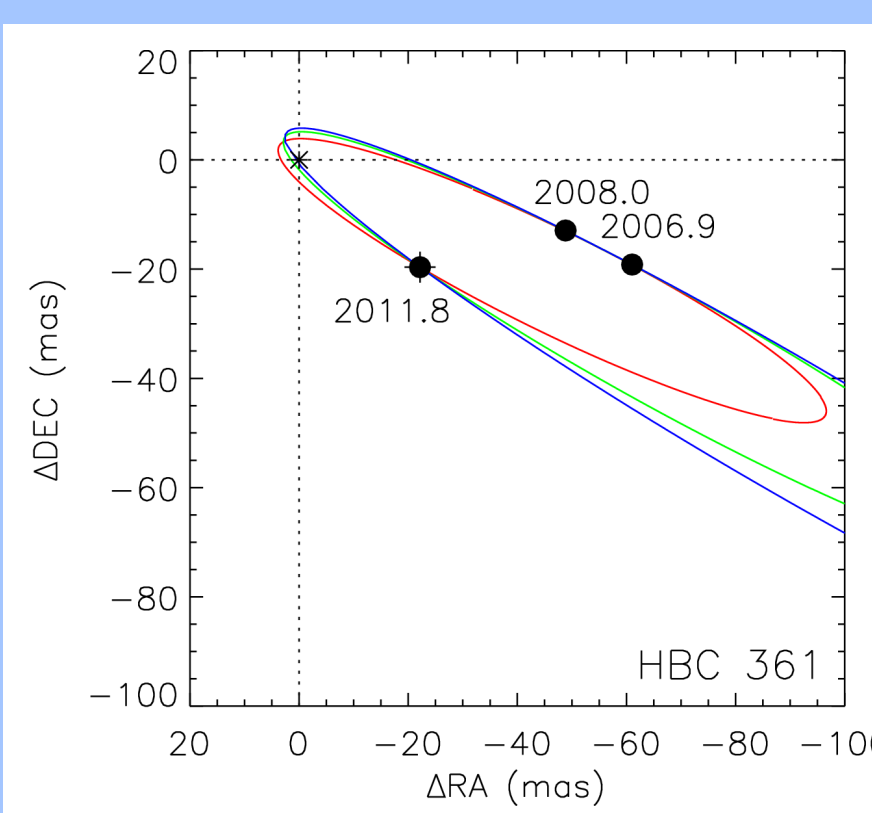


Figure 10 - Orbital motion for HBC 361. Black circles are our NIRC2 measurements. Overplotted are three example orbits at periods of 25 (red), 40 (green), and 60 yr (blue) that are consistent with the observed motion. A statistical analysis of orbital solutions that fit the data indicates that the 1σ confidence interval extends from 10 to 230 yr.

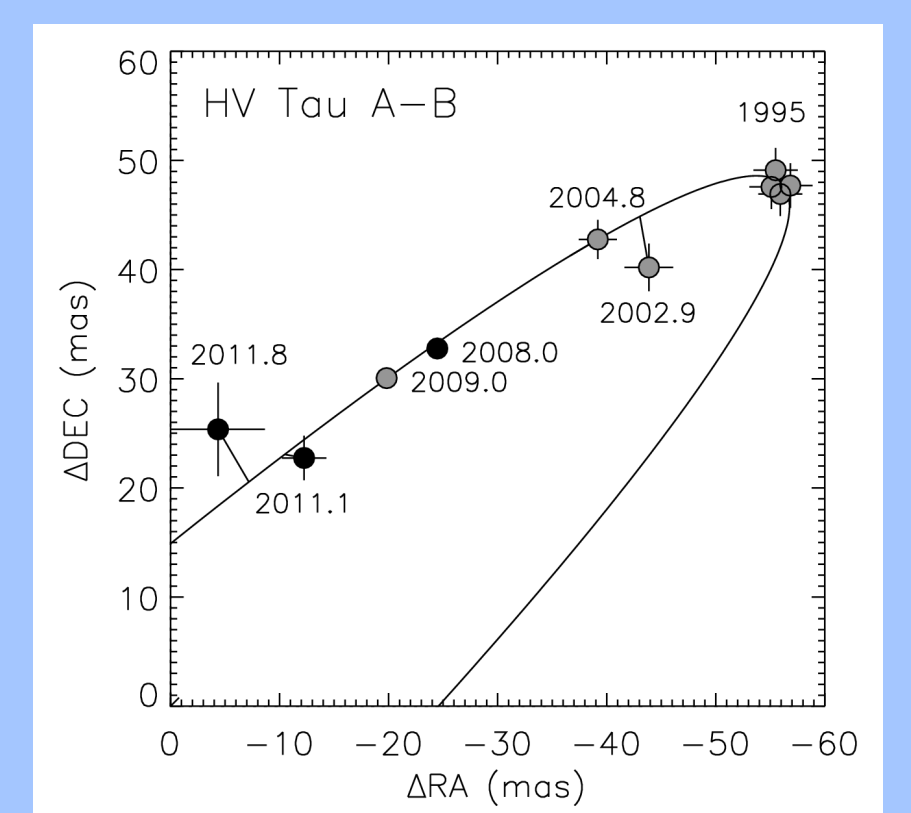


Figure 11 - Orbital motion for HV Tau A-B. Black circles are our NIRC2 measurements. Grey circles are from the literature (S92, S96, MB00, Du10, Kr11). Overplotted is an example orbit of 200 yr that is consistent with the data. A statistical analysis of orbital solutions that fit the data indicates that $P > 27$ yr.

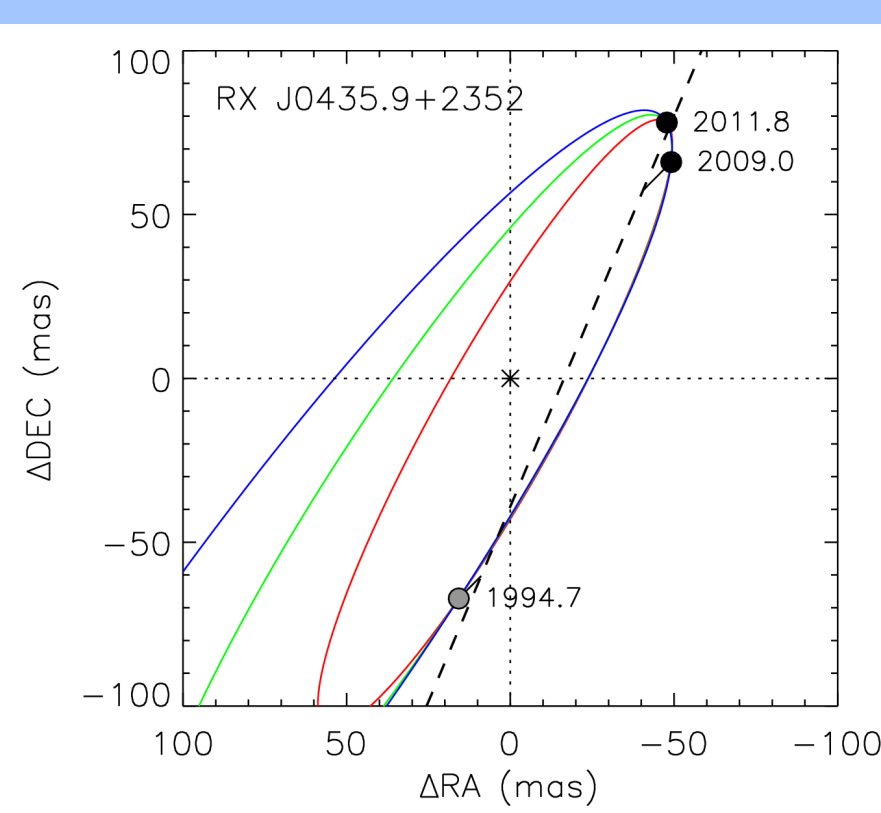


Figure 12 - Orbital motion for RX J0435.9+2352. Black circles are our NIRC2 measurements. Grey circle is from KL98. The dashed line shows a fit for linear motion. Overplotted are orbits at periods of 50 (red), 100 (green), and 200 yr (blue) that are consistent with the observed motion. A statistical analysis of orbital solutions that fit the data indicates that $P > 20$ yr.

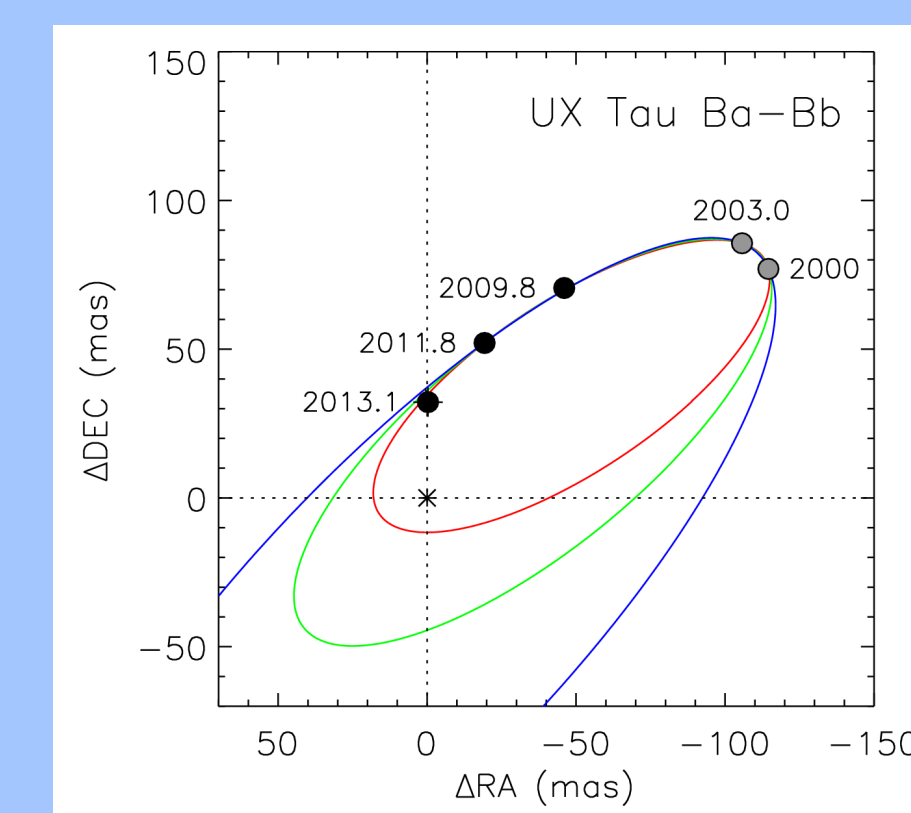


Figure 13 - Orbital motion for UX Tau Ba-Bb. Black circles are our NIRC2 measurements. Grey circles are from the literature (Du99, Co06). Overplotted are orbits at periods of 25 (red), 40 (green), and 100 yr (blue). A statistical analysis of orbital solutions that fit the data indicates that $P > 20$ yr. UX Tau B is located 5.9" to the west of UX Tau A. UX Tau C is located 2.7" south of UX Tau A.

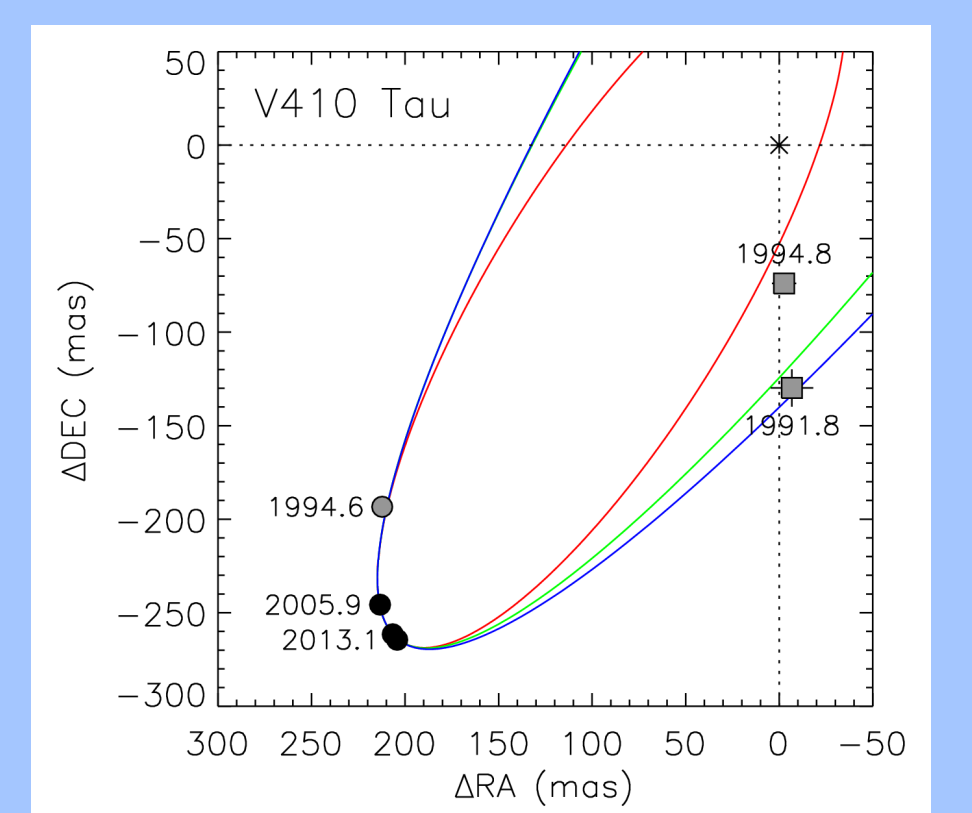


Figure 14 - Orbital motion for V410 Tau. Black circles are our NIRC2 measurements. Grey circle is from WG01. Overplotted are orbits at periods of 100 (red), 200 (green), and 300 yr (blue). A statistical analysis of orbital solutions that fit the data indicates that $P > 68$ yr. The grey squares are companion B detected by Gh95. We did not detect V410 Tau B in our AO images.

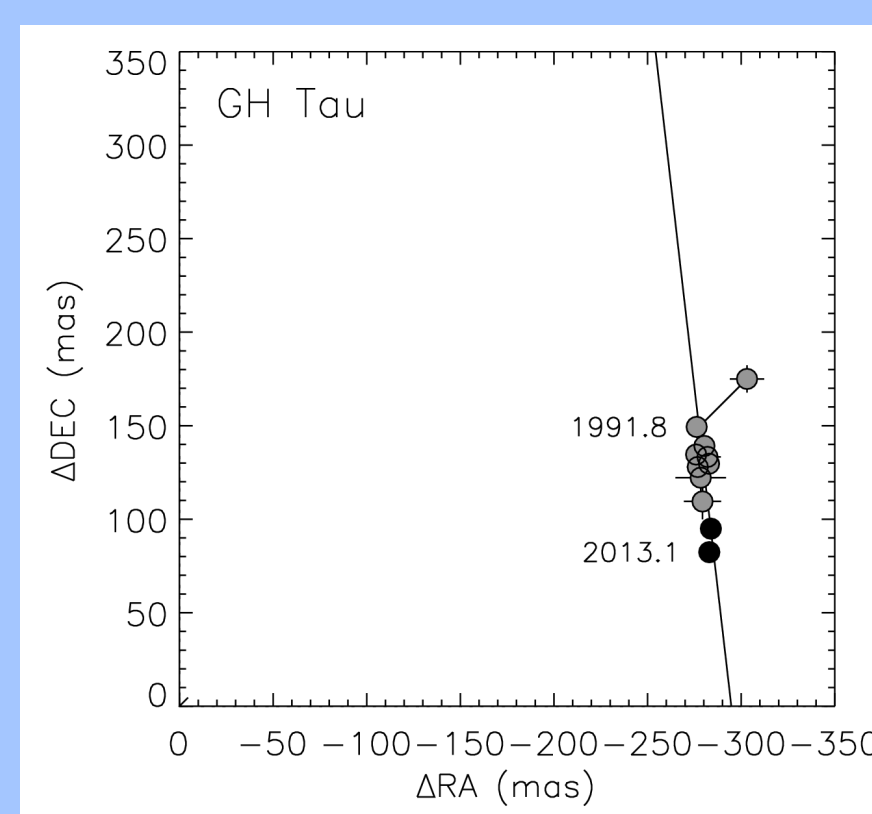


Figure 15 - Orbital motion for GH Tau. Black circles are our NIRC2 measurements. Grey circles are from the literature (Lei93, Gh95, WG01, W0101, HK03). The solid line shows a fit for linear motion. A statistical analysis of orbital solutions that fit the data indicates that $P > 95$ yr.

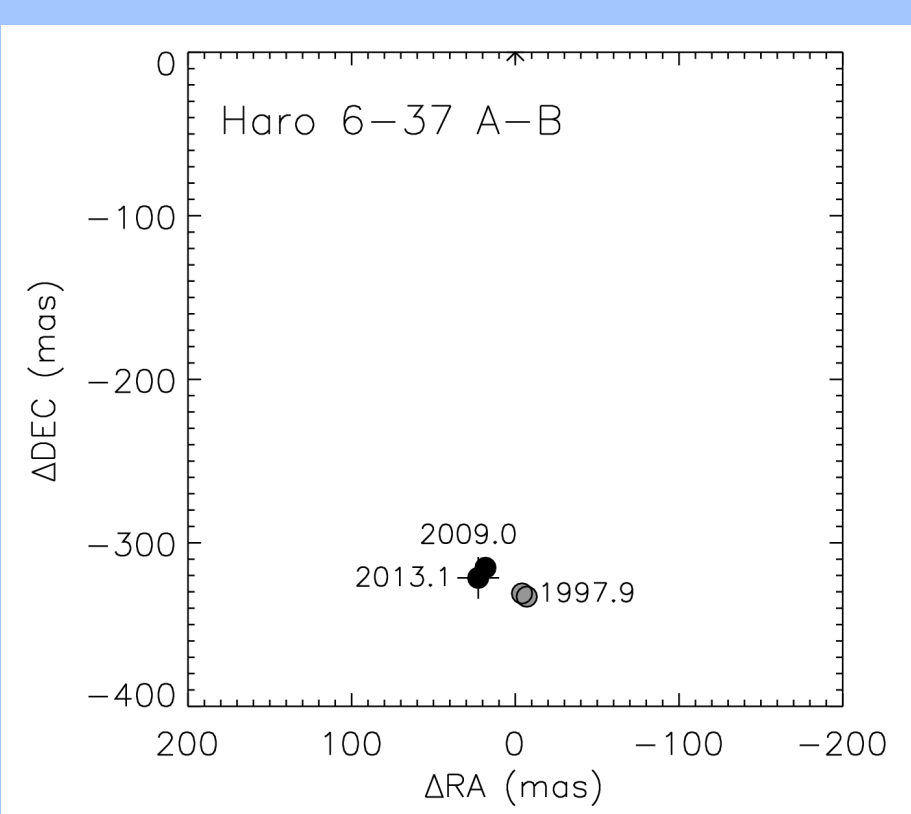


Figure 16 - Orbital motion for Haro 6-37 A-B. Black circles are our NIRC2 measurements. Grey circles are from the literature (Du99, Ri99). The close pair is moving slowly relative to each other, so we cannot yet place limits on the orbital motion. The faint tertiary, Haro 6-37 C, is located 2.7" to the northeast of A.

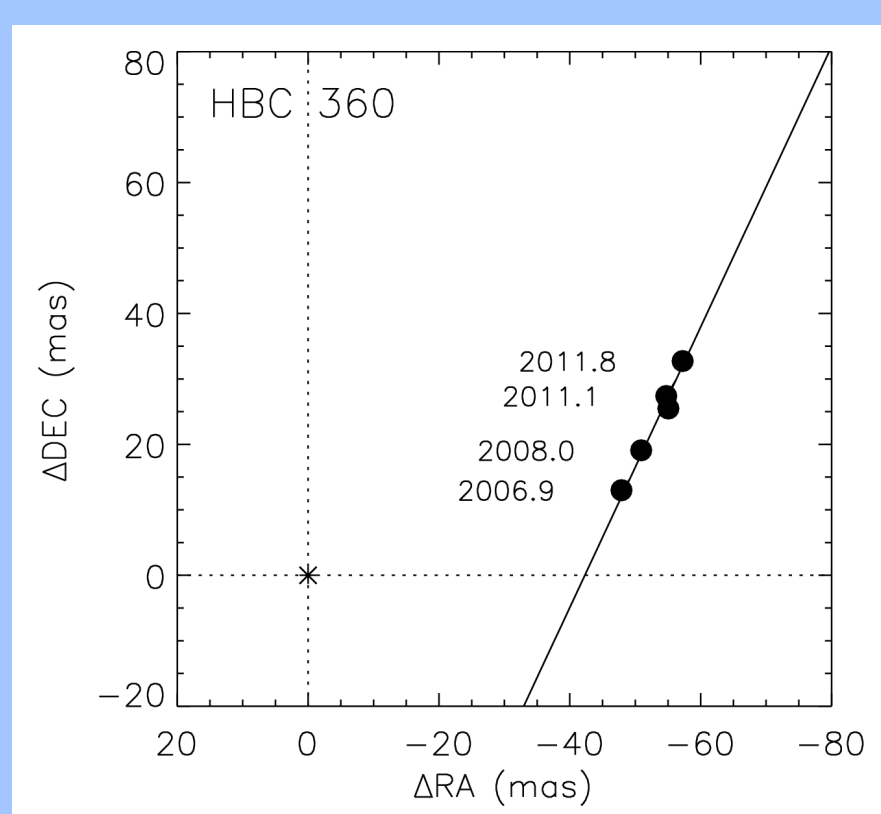


Figure 17 - Orbital motion for HBC 360. Black circles are our NIRC2 measurements. The solid line shows a fit for linear motion. A statistical analysis of orbital solutions that fit the data indicates that $P > 15$ yr.

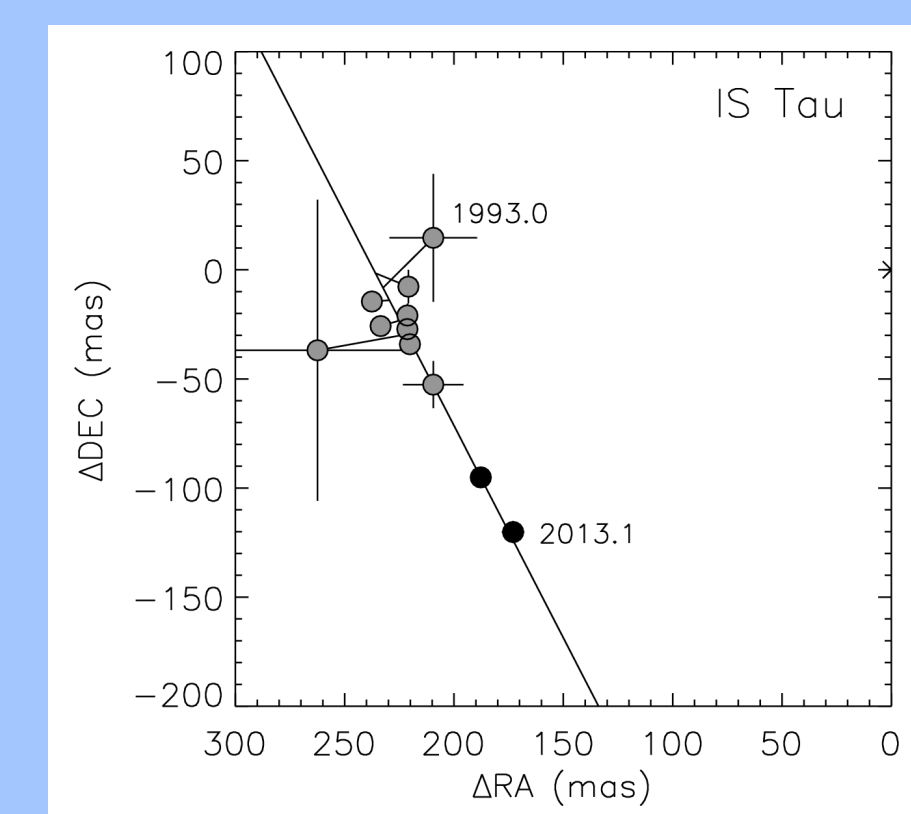


Figure 18 - Orbital motion for IS Tau. Black circles are our NIRC2 measurements. Grey circles are from the literature (Lei93, Gh93, WG01, W0101, HK03). The solid line shows a fit for linear motion. A statistical analysis of orbital solutions that fit the data indicates that $P > 57$ yr.

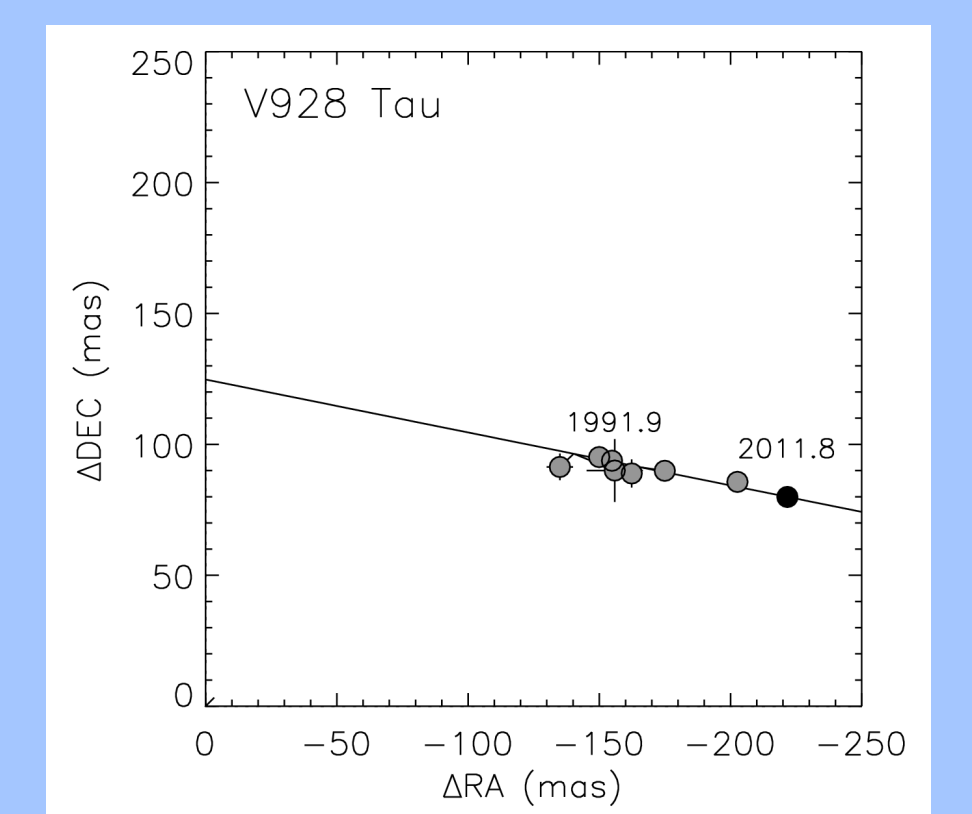


Figure 19 - Orbital motion for V928 Tau. Black circles are our NIRC2 measurements. Grey circles are from the literature (Lei93, Gh95, S96, WG01, KH12). The solid line shows a fit for linear motion. A statistical analysis of orbital solutions that fit the data indicates that $P > 58$ yr.